

Interacting electron-phonon system

1) non-interacting electron system & non-interacting phonon system

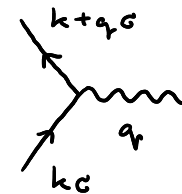
$$H_0 = \sum_{k\sigma} \epsilon_{k\sigma} \hat{c}_{k\sigma}^\dagger \hat{c}_{k\sigma} + \sum_{q\lambda} \omega_{q\lambda} \hat{a}_{q\lambda}^\dagger \hat{a}_{q\lambda} \rightarrow \text{single band/branch for simplicity}$$

bare propagators $\xrightarrow{k\sigma}$ \xleftarrow{q}

$$S_0 = -\frac{1}{\hbar} \langle T \{ \hat{c}_{k\sigma}^\dagger(z) \hat{c}_{k\sigma} \} \rangle \quad D_0 = -\frac{1}{\hbar} \langle T \{ (\hat{a}_q + \hat{a}_{-q}^\dagger)_z (\hat{a}_q + \hat{a}_{-q}^\dagger)_0 \} \rangle$$

2) electron-phonon interaction

$$H_{e-p} = \sum_{kq\sigma} M_{kq\sigma} \hat{c}_{k+q\sigma}^\dagger \hat{c}_{k\sigma} (\hat{a}_q + \hat{a}_{-q}^\dagger)$$



- electron renormalization \rightarrow polarons **renormalized propagator** \Rightarrow
- phonon renormalization \rightarrow modified sound velocity, Kohn anomalies \approx
- effective e-e interaction \rightarrow Cooper pairing & SC $\nearrow \nwarrow$

① Phonons and e-ph coupling

- Born-Oppenheimer approximation

$$H = \underbrace{T_e + V_{e-e}}_{\text{electrons}} + \underbrace{T_n + V_{n-n}}_{\text{nuclei}} + \underbrace{V_{e-n}}_{\text{mutual interaction}}$$

$m_e \ll M \rightarrow$ nuclei are slow to react, lattice dynamics captured by

$$H_{\text{lattice}} = T_n + V_{n-n} + E_{GS}[\text{lattice config.}] = \sum_i \frac{p_i^2}{2M_i} + \frac{1}{2} \sum_{i \neq j} \frac{z_\alpha z_\beta e^2}{|R_i - R_j|} + E_{GS}[R_1 \dots R_N]$$

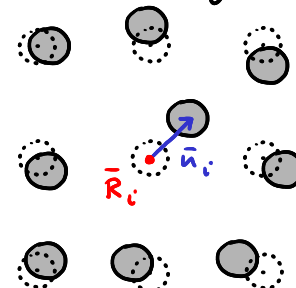
- harmonic approximation

consider small deviations from ideal lattice positions and perform Taylor expansion

$$H_{\text{harm}} = \sum_i \frac{p_i^2}{2M_i} + V_0 + \frac{1}{2} \sum_{i,j} \bar{u}_i^\top V_{ij} \bar{u}_j$$

quadratic Hamiltonian

$$(V_{ij})_{\alpha\beta} = \frac{\partial^2 V}{\partial u_i^\alpha \partial u_j^\beta}$$



- Fourier transform and diagonalization

$$\bar{u}_R = \sum_q e^{i\vec{q} \cdot \vec{R}} \bar{u}_q = \frac{1}{\sqrt{N}} \sum_{q,\lambda} \sqrt{\frac{\hbar}{M\omega_{q\lambda}}} \bar{\epsilon}_{q\lambda} e^{i\vec{q} \cdot \vec{R}} Q_{q\lambda}$$

↑
polarization vector ↑
eigen coordinate

(consider 1 atom/u.c.)

$$\rightarrow H_{\text{harm}} = \sum_{q,\lambda} \frac{1}{2} \hbar \omega_{q\lambda} (P_{q\lambda} P_{-q\lambda} + \omega_{q\lambda}^2 Q_{q\lambda} Q_{-q\lambda})$$

"independent" harmonic oscillators

- quantization $[Q_{q_i}, P_{q'_i}] = i\hbar \delta_{qq'}$

$$\begin{aligned} \hat{a}_q &= \frac{1}{\sqrt{2}} (Q_q + i P_q^+) \\ \hat{a}_q^+ &= \frac{1}{\sqrt{2}} (Q_q^+ - i P_q) = \frac{1}{\sqrt{2}} (Q_{-q} - i P_{-q}^+) \end{aligned} \quad \left. \right\} \rightarrow$$

non interacting bosons

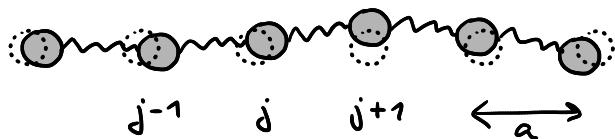
$$H_{\text{harm}} = \sum_{q,\lambda} \hbar \omega_{q\lambda} \hat{a}_{q\lambda}^+ \hat{a}_{q\lambda} + E_0$$

$$[\hat{a}_{q\lambda}, \hat{a}_{q'\lambda'}^+] = \delta_{qq'} \delta_{\lambda\lambda'}$$

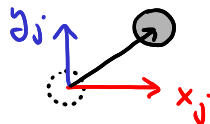
quantized deviation from lattice position

$$\bar{u}_R = \frac{1}{\sqrt{N}} \sum_{q,\lambda} \sqrt{\frac{\hbar}{2M\omega_{q\lambda}}} \bar{\epsilon}_{q\lambda} e^{i\vec{q} \cdot \vec{R}} (\hat{a}_{q\lambda} + \hat{a}_{-q\lambda}^+)$$

- example - monoatomic linear chain



deviation



spring stiffness

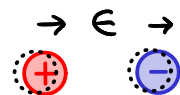
$$H = \sum_j \frac{1}{2M} p_j^2 + \frac{1}{2} \sum_j \left\{ \alpha_{\parallel} (x_j - x_{j-1})^2 + \alpha_{\perp} [(y_j - y_{j-1})^2 + (z_j - z_{j-1})^2] \right\}$$

$$= \sum_q \sum_{\lambda=1}^3 \hbar \omega_{q\lambda} \hat{a}_{q\lambda}^+ \hat{a}_{q\lambda}$$

$$\omega_{q1} = \sqrt{\frac{2\alpha_{\parallel}}{M}(1 - \cos qa)}$$

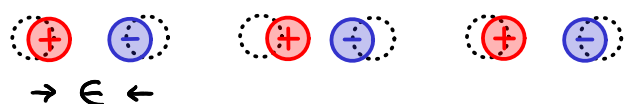
$$\omega_{q2,3} = \sqrt{\frac{2\alpha_{\perp}}{M}(1 - \cos qa)}$$

- example - diatomic linear chain

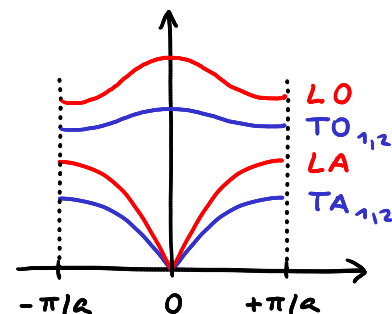
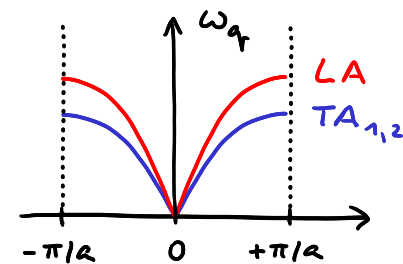


LA acoustic

$$\vdots \rightarrow \vdots \rightarrow \vdots \rightarrow \vdots \rightarrow \vdots e^{iqR}$$



LO optical



- electron-phonon interaction

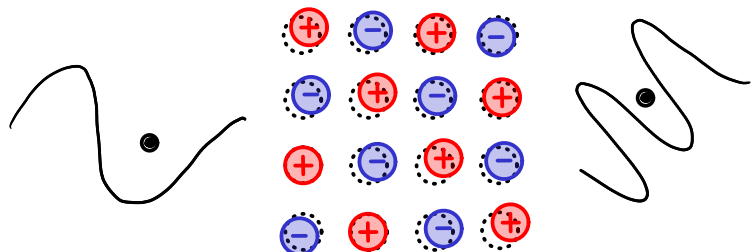
phonons modulate the lattice potential & electrons scatter on this modulation

$$H_{el} = T_e + V_{e-e} + \sum_i V_{at} [\hat{r}_i - (R + \hat{u}_R)] \rightarrow \approx V_{at}(\hat{r} - R) + \hat{u}_R \cdot \nabla V(\hat{r} - R)$$

electrons ↑ phonons ↑

$$H_{e-ph} = \sum_i \hat{u}_R \cdot \nabla V_{at} (\hat{r} - R)$$

Fourier
→



$$H_{e-ph} = \sqrt{N} \sum_{kG} \sum_{q\lambda} \sum_G \sqrt{\frac{\hbar}{2M\omega_{q\lambda}}} (q + G) \cdot \epsilon_{q\lambda} V_{q+G} \hat{c}_{k+q+G,G}^+ \hat{c}_{kG} (\hat{a}_{q\lambda} + \hat{a}_{-q\lambda}^+)$$

1) $G=0$ normal processes , $G \neq 0$ Umklapp processes - neglected

2) $q \cdot \epsilon_{q\lambda} \rightarrow$ transverse phonons do not couple

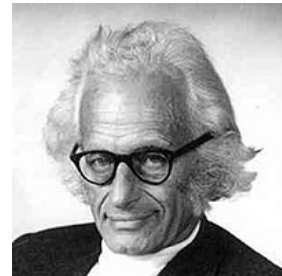
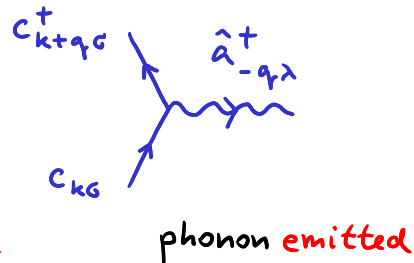
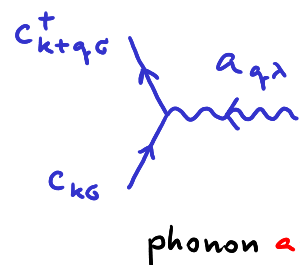
Fröhlich Hamiltonian

Fanny Frida (née Schwarz)

Jakob Julius Fröhlich

$$H_{e-ph} = \sum_{k\sigma} \sum_{q\lambda} M_{q\lambda} \hat{c}_{k+q,\sigma}^+ \hat{c}_{k\sigma} (\hat{a}_{q\lambda} + \hat{a}_{-q\lambda}^+)$$

$$(\text{Hermitian} \rightarrow M_{q\lambda}^* = M_{-q\lambda})$$

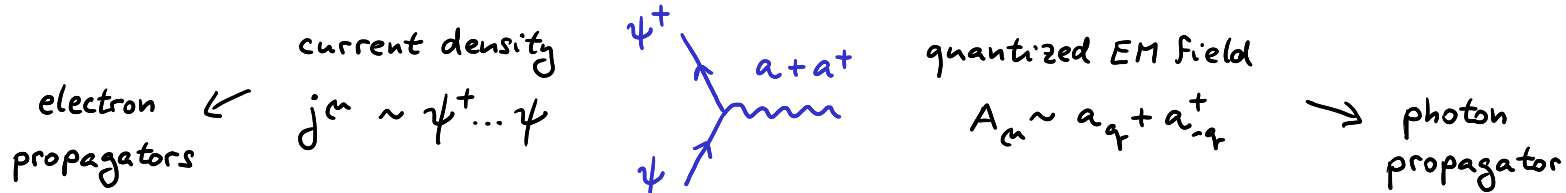


Herbert Fröhlich (1905–1991)

- analogy to QED

coupling of electrons to EM fields:

$$\hat{H}_{int} = S\varphi - \bar{j} \cdot \bar{A} = -j^{\mu} A_{\mu}$$



② Propagators and diagrams

- phonon field (\sim deviation)

$$\hat{\phi}_{q\lambda} = \hat{a}_{q\lambda} + \hat{a}_{-q\lambda}^+ \quad \text{conjugate} \quad \hat{\phi}_{q\lambda}^+ = \hat{a}_{q\lambda}^+ + \hat{a}_{-q\lambda} = \hat{\phi}_{-q\lambda}$$

$$\rightarrow e\text{-ph coupling of the form} \sum M_{q\tau} c_{k+q}^+ c_k \phi_{q\tau}$$

- bare phonon propagator

$$\mathcal{D}_0(q\lambda, \tau) = -\frac{1}{\hbar} \langle T \{ \hat{\phi}_{q\lambda}(\tau) \hat{\phi}_{-q\lambda}(0) \} \rangle_0 \quad \text{non-interacting} \quad \hat{H}_0 = \sum_{q\lambda} \hbar \omega_{q\lambda} \hat{a}_{q\lambda}^+ \hat{a}_{q\lambda}$$

$$\begin{aligned} \text{single branch} \quad -\hbar \mathcal{D}_0(q, \tau) &= \left\langle e^{\frac{\tau}{\hbar} \hat{H}_0} (a_q + a_{-q}^+) e^{-\frac{\tau}{\hbar} \hat{H}_0} (a_{-q} + a_q^+) \right\rangle_0 \mathcal{G}(\tau) + \\ &+ \left\langle (a_{-q} + a_q^+) e^{\frac{\tau}{\hbar} \hat{H}_0} (a_q + a_{-q}^+) e^{-\frac{\tau}{\hbar} \hat{H}_0} \right\rangle_0 \mathcal{G}(-\tau) = \end{aligned}$$

$$\left. \begin{aligned} e^{\frac{\tau}{\hbar} \hat{H}_0} a_q e^{-\frac{\tau}{\hbar} \hat{H}_0} &= e^{-\omega_q \tau} a_q \\ e^{\frac{\tau}{\hbar} \hat{H}_0} a_{-q}^+ e^{-\frac{\tau}{\hbar} \hat{H}_0} &= e^{\omega_q \tau} a_{-q}^+ \end{aligned} \right\} \rightarrow = [e^{\omega_q \tau} \langle a_{-q}^+ a_{-q} \rangle_0 + e^{-\omega_q \tau} \langle a_q a_q^+ \rangle_0] \mathcal{G}(\tau) + [e^{-\omega_q \tau} \langle a_q^+ a_q \rangle_0 + e^{\omega_q \tau} \langle a_{-q} a_{-q}^+ \rangle_0] \mathcal{G}(-\tau)$$

$$\mathcal{D}_o(q, \tau > 0) = -\frac{1}{\hbar} [e^{\omega_q \tau} n_q + e^{-\omega_q \tau} (1 + n_q)]$$

Bose-Einstein statistics

$$n_q = N_B(\hbar \omega_q) = \frac{1}{e^{\beta \hbar \omega_q} - 1}$$

Matsubara coefficients (utilizing bosonic symmetry of \mathcal{D}_o)

$$\begin{aligned} \mathcal{D}_o(q, i\omega_m) &= \int_0^{\beta} d\tau \mathcal{D}_o(q, \tau) e^{i\omega_m \frac{\tau}{\hbar}} = - \int_0^{\beta} d\frac{\tau}{\hbar} e^{(\hbar \omega_q + i\omega_m) \frac{\tau}{\hbar}} n_q + e^{(-\hbar \omega_q + i\omega_m) \frac{\tau}{\hbar}} \\ &= -\frac{e^{\beta \hbar \omega_q} - 1}{i\omega_m + \hbar \omega_q} n_q - \frac{e^{-\beta \hbar \omega_q} - 1}{i\omega_m - \hbar \omega_q} (n_q + 1) = \frac{1}{i\omega_m - \hbar \omega_q} - \frac{1}{i\omega_m + \hbar \omega_q} = \frac{2\hbar \omega_q}{(i\omega_m)^2 - (\hbar \omega_q)^2} \end{aligned}$$

• Lehmann representation

retarded propagator

$$\mathcal{D}_o(q, i\omega_m) = \int dE \frac{B(q, E)}{i\omega_m - E}$$

$$\mathcal{D}_{\text{ret}}(q, E) = \mathcal{D}_o(q, i\omega_m \rightarrow E + i0^+) = \int dE' \frac{B(q, E')}{E + i0^+ - E'}$$

spectral function

$$B(q, E) = \delta(E - \hbar \omega_q) - \delta(E + \hbar \omega_q) = -\frac{1}{\pi} \text{Im } \mathcal{D}_{\text{ret}}(q, E)$$

odd function of E
(generic for bosonic GFs)

- Dyson perturbation formula for single-particle propagator

$$H_{e-ph}(\tau_n) = \sum_{kGq} M_q \hat{c}_{k+qG}^+(\tau_n^+) \hat{c}_{k\sigma}(\tau_n) \phi_q(\tau_n)$$

↓

$$G(\tau \geq 0) = -\frac{1}{\hbar} \frac{\langle T \left\{ \sum_{n=0}^{\infty} \left(-\frac{1}{\hbar}\right)^n \frac{1}{n!} \int_0^{\tau_1} d\tau_1 \int_0^{\tau_2} d\tau_2 \cdots \int_0^{\tau_n} d\tau_n \tilde{V}(\tau_1) \tilde{V}(\tau_2) \cdots \tilde{V}(\tau_n) \hat{c}_{k\sigma}(\tau) \hat{c}_{k\sigma}^+(0) \right\} \rangle}{\langle T \left\{ \sum_{n=0}^{\infty} \left(-\frac{1}{\hbar}\right)^n \frac{1}{n!} \int_0^{\tau_1} d\tau_1 \int_0^{\tau_2} d\tau_2 \cdots \int_0^{\tau_n} d\tau_n \tilde{V}(\tau_1) \tilde{V}(\tau_2) \cdots \tilde{V}(\tau_n) \right\} \rangle}$$

$\langle \text{expression involving } \hat{c}, \hat{c}^+, \hat{\phi} \rangle$ Wick's theorem → products of non-interacting G_0 and D_0

D_0 contains two $\hat{\phi}$ → only even $n = 2k$ - diagrams with k phonon lines

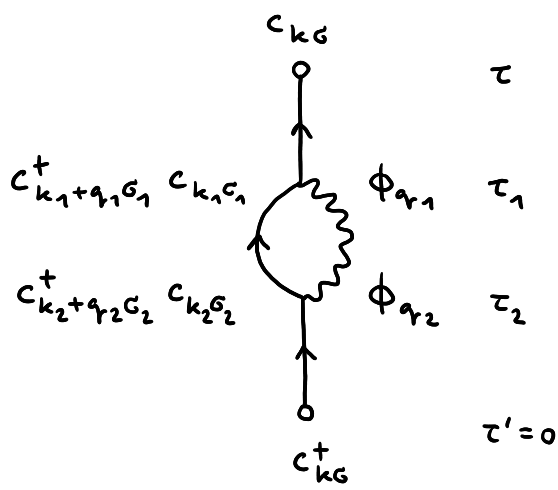
- cancellation of disconnected diagrams

- compensation of $\frac{1}{n!}$ by permuting the $\tau_1 \dots \tau_n$ labels

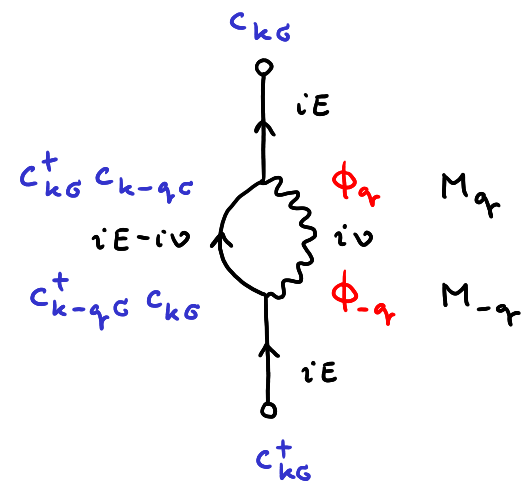
$n=2$ example

$$\langle T \left\{ \sum_{k_1 G_1 q_1} \hat{c}_{k_1 + q_1 G_1}^+ (\tau_1^+) \hat{c}_{k_1 G_1} (\tau_1) \phi_{q_1} (\tau_1) \sum_{k_2 G_2 q_2} \hat{c}_{k_2 + q_2 G_2}^+ (\tau_2^+) \hat{c}_{k_2 G_2} (\tau_2) \phi_{q_2} (\tau_2) \hat{c}_{k_0} (\tau) \hat{c}_{k_0}^+ (0) \right\} \rangle_0$$

$\overbrace{\hspace{10em}}$ $\sim H_{e-ph}(\tau_1)$ $\overbrace{\hspace{10em}}$ $\sim H_{e-ph}(\tau_2)$
 $\boxed{g_o}$ $\boxed{g_o}$ $\boxed{D_o}$ $\boxed{g_o}$



momentum
+
spin
+
M. energy
conservation



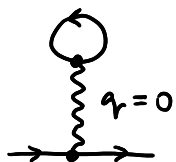
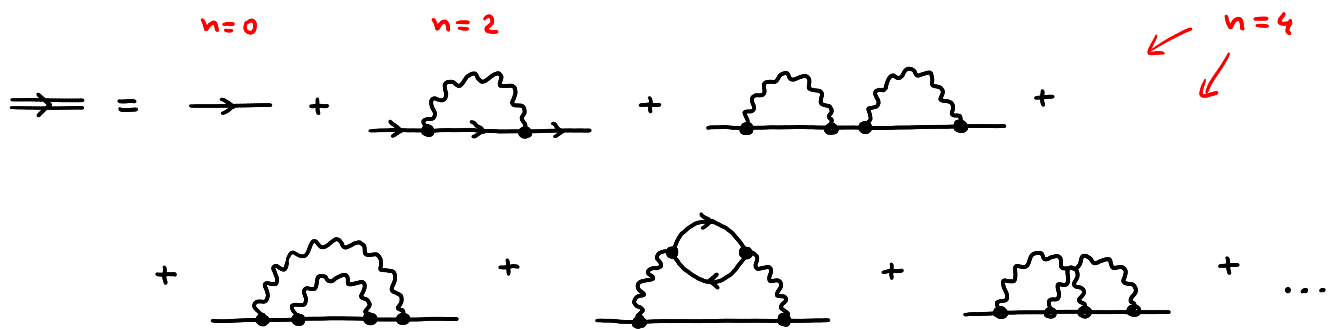
- new diagrammatic rules

$$\text{~~~~} -\mathcal{D}_0(q_r, i\nu) \\ q_r, i\nu$$

$$\text{~~~~} -\mathcal{D}(q_r, i\nu) \\ q_r, i\nu$$

$$k+q_r \quad k \quad q_r \\ -M_{q_r}$$

- diagrammatic expansion of electron propagator



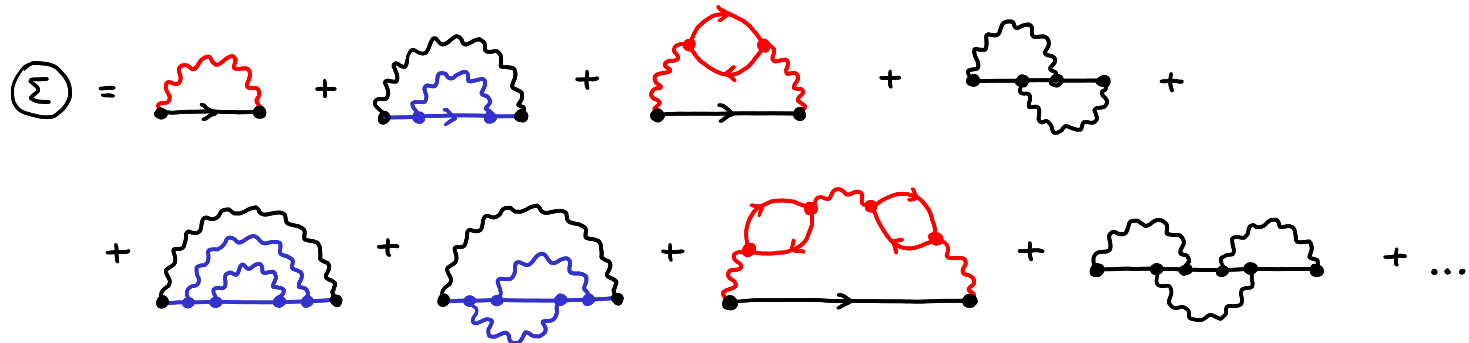
and similar diagrams drop due to $M_{q_r} \rightarrow 0 \rightarrow 0$

(screened Coulomb interaction \rightarrow finite V_{q_r} killed by $q_r \cdot E_{q_r}$)

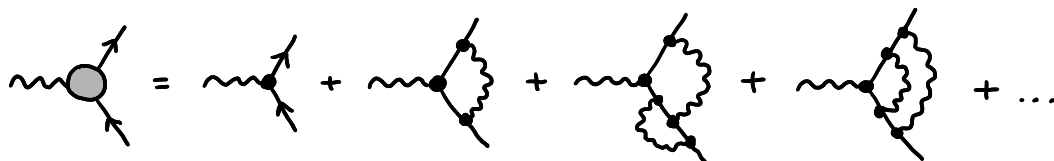
③ Electron renormalization by phonons - polarons

- electron selfenergy

Dyson equation: $\Rightarrow = \rightarrow + \rightarrow \circlearrowleft \rightarrow$



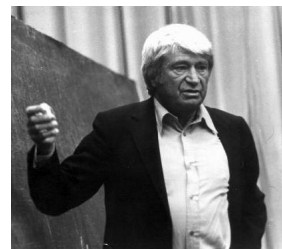
- vertex corrections & Migdal's theorem



**dressed
vertex**

**bare
vertex**

$$\text{Migdal (1958): } \bullet = \bullet \left[1 + \sigma \left(\sqrt{\frac{m}{M}} \right) \right]$$



Arkady Migdal
(11.3.1911 Lida, Belarus
–9.2.1991 Princeton, US)

- approximations

$$\Sigma = \text{Diagram} + \text{Diagram} + \text{Diagram} + \text{Diagram} + \text{Diagram} + \text{Diagram} + \dots$$

$$\Sigma = \text{Diagram} \approx \text{Diagram} \approx \text{Diagram} \approx \text{Diagram}$$

vertex corrections neglected selfconsistent Born approx. 1st Born approximation

- evaluation of the selfenergy

$$\Sigma = \text{Diagram}$$

$\overset{\text{q}_f, i\nu}{\curvearrowright}$
 k_i, iE $k - q_f, iE - i\nu$ k_f, iE

$$-\Sigma(k, iE) = \sum_q \frac{1}{\beta} \sum_{i\nu} |M_{qf}|^2 G(k-q, iE-i\nu) \mathcal{D}(q, i\nu)$$

Lehmann: $G(k, iE) = \int dE' \frac{A(k, E')}{iE - E'}$ ← spectral functions

$$\mathcal{D}(q, i\nu) = \int d\omega \frac{B(q, \omega)}{i\nu - \omega}$$
 ← functions

$$\Sigma(k, iE) = - \sum_q |M_{qf}|^2 \int d\omega \int dE B(q, \omega) A(k-q, E') \frac{1}{\beta} \sum_{i\nu} \frac{1}{iE - i\nu - E'} \frac{1}{i\nu - \omega}$$

$$\text{sum } \frac{1}{\beta} \sum_{iv} \frac{1}{iE - iv - E'} \frac{1}{iv - \omega} = \frac{1}{\beta} \sum_{iv} f(iv) \text{ evaluated using } \oint f(z) N_B(z) dz = 0$$

$\sum \text{residues} = 0$ & N_B has poles at the set of iv

↑ drops as $\frac{1}{|z|^2}$

$\rightarrow \text{sum} \sim \sum \text{residues of } f(z) N_B(z) \text{ at poles of } f(z)$

Final result

$$\Sigma(k, iE) = \sum_q |M_q|^2 \int d\omega \int dE B(q, \omega) A(k-q, E') \frac{1 - n_F(E') + N_B(\omega)}{iE - E' - \omega}$$

• simplified model - Holstein polaron

- single electron (μ at bottom of the el. band $\rightarrow \varepsilon_k \geq 0, A(k, E < 0) = 0$)

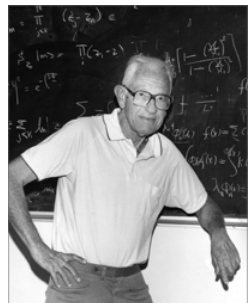
- dispersionless bare LO phonon $\rightarrow B(q, \omega) = \delta(\omega - \omega_0) - \delta(\omega + \omega_0)$

- constant e-ph coupling $M_q = g/\sqrt{N}$

- zero temperature $T=0$ implying

$$n_F(\varepsilon) = \begin{cases} 0 & \varepsilon > 0 \\ 1 & \varepsilon < 0 \end{cases} \quad N_B(\omega) = \begin{cases} 0 & \omega > 0 \\ -1 & \omega < 0 \end{cases}$$

↑
Holstein model



Theodore David Holstein (1915-1985)

$$\Sigma(k, iE) = \sum_q \underbrace{|M_q|^2}_{g^2/N} \int d\omega \int dE' \underbrace{B(q, \omega)}_{\delta(\omega - \omega_0) - \delta(\omega + \omega_0)} A(k-q, E') \frac{\frac{1}{iE - E' - \omega} \overset{\circ}{n_F}(E') + N_B(\omega)}{\rightarrow \omega > 0 \text{ only}}$$

$$= \frac{g^2}{N} \sum_q \int dE' A(k-q, E') \frac{1}{iE - E' - \omega_0} \rightarrow k\text{-independent selfenergy}$$

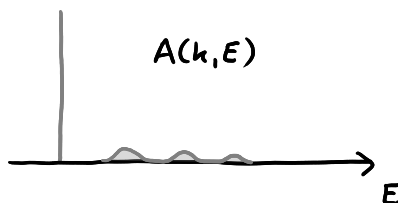
retarded real axis version $\Sigma(E) = \frac{g^2}{N} \sum_k \int dE' \frac{A(k, E')}{E + i0^+ - E' - \omega_0} = \frac{g^2}{N} \sum_k G_{\text{ret}}(k, E - \omega_0)$

\rightarrow implicit equation

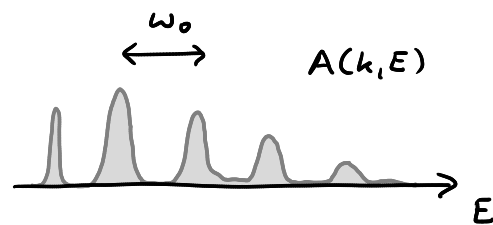
$$\Sigma(E) = \frac{g^2}{N} \sum_k \frac{1}{E - \omega_0 + i0^+ - (\varepsilon_k - \mu) - \Sigma(E - \omega_0)}$$

$$G_{\text{ret}}(k, E) = \frac{1}{E + i0^+ - (\varepsilon_k - \mu) - \Sigma(E)}$$

Small g
WC



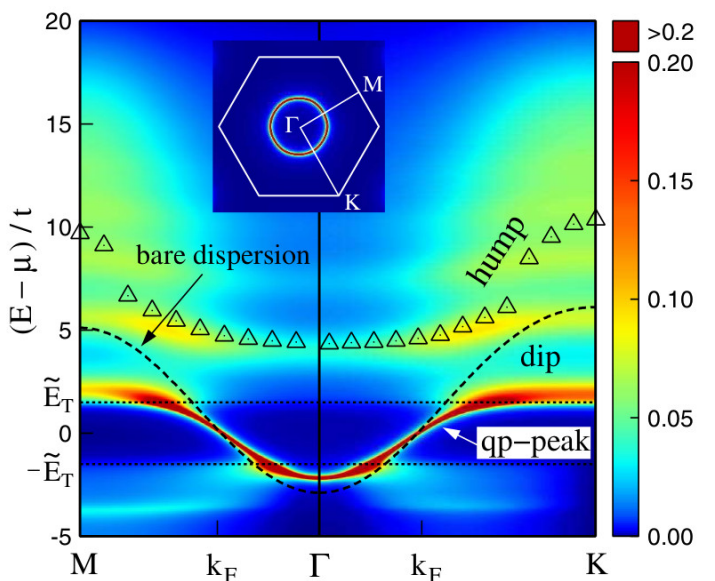
large g
SC



• polaron based on spin excitations

$$H_{\tilde{t}} = -\frac{\tilde{t}}{\sqrt{3}} \sum_{ij} [T_{+1\gamma i}^+ f_{j\downarrow}^+ f_{i\uparrow} - T_{-1\gamma i}^+ f_{j\uparrow}^+ f_{i\downarrow}]$$

$$T_{0\gamma i}^+ \frac{1}{\sqrt{2}} (f_{j\uparrow}^+ f_{i\uparrow} - f_{j\downarrow}^+ f_{i\downarrow}) + \text{h.c.}]$$



Spin Polaron Theory for the Photoemission Spectra of Layered Cobaltates

Jiří Chaloupka^{1,2} and Giniyat Khalilullin¹

¹Max-Planck-Institut für Festkörperforschung, Heisenbergstrasse 1, D-70569 Stuttgart, Germany

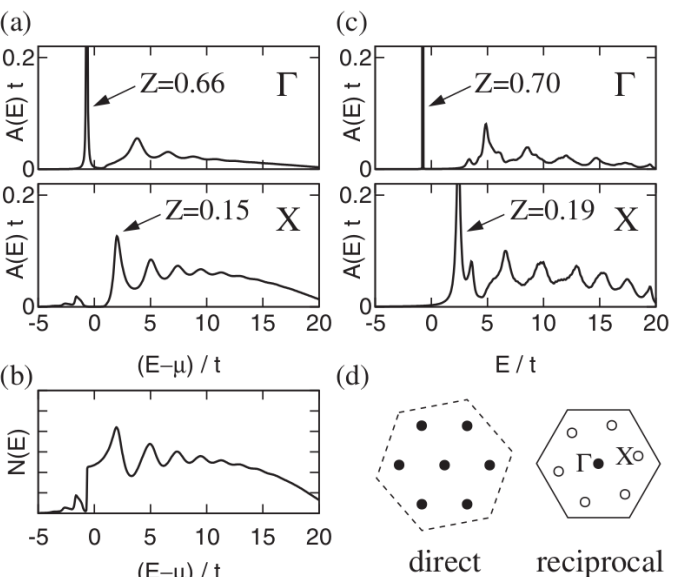
²Department of Condensed Matter Physics, Masaryk University, Koliářská 2, 61137 Brno, Czech Republic

(Received 3 August 2007; published 20 December 2007)

Recently, strong reduction of the quasiparticle peaks and pronounced incoherent structures have been observed in the photoemission spectra of layered cobaltates. Surprisingly, these many-body effects are found to increase near the band-insulator regime. We explain these unexpected observations in terms of a novel spin-polaron model for CoO_2 planes, which is based on a fact of the spin-state quasidegeneracy of Co^{3+} ions in oxides. Scattering of the photoholes on spin-state fluctuations suppresses their coherent motion. The observed "peak-dip-hump" type line shapes are well reproduced by the theory.

DOI: 10.1103/PhysRevLett.99.256406

PACS numbers: 71.27.+a, 72.10.Di, 79.60.-i

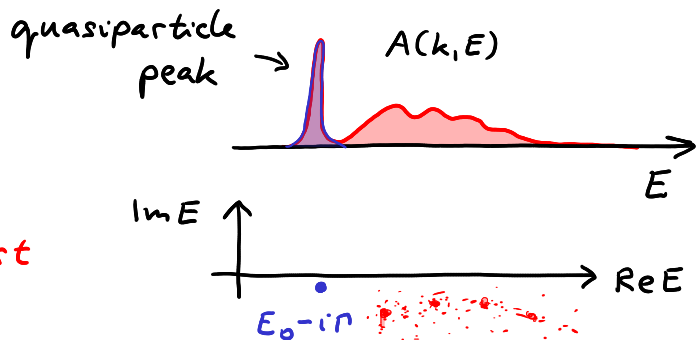


- quasiparticle weight and lifetime

$$G_{\text{ret}}(k, E) = \frac{1}{E + i0^+ - (\varepsilon_k - \mu) - \Sigma(k, E)}$$

$$\approx \frac{Z}{E - (E_0 - i\Gamma)} + \text{incoherent part}$$

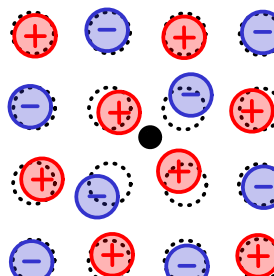
$$A = -\frac{1}{\pi} \text{Im } G_{\text{ret}} = Z \frac{1}{\pi} \frac{\Gamma}{(E - E_0)^2 + \Gamma^2} + \text{incoherent part}$$



- intuitive picture of a polaron

$$\Rightarrow = \rightarrow + \rightarrow \bullet \rightarrow \bullet \rightarrow + \quad + \quad \begin{array}{c} \nearrow \\ \searrow \end{array} \quad + \quad \rightarrow \bullet \rightarrow \bullet \rightarrow$$

electron accompanied by a cloud of excitations



Соломон Ісаакович Пекар
(1917 Київ - 1985 Київ)



Лев Давидович Ландау
(1908 Bakı - 1968 Москва)

• experiment - polarons in 2D electron liquid at SrTiO_3 interfaces

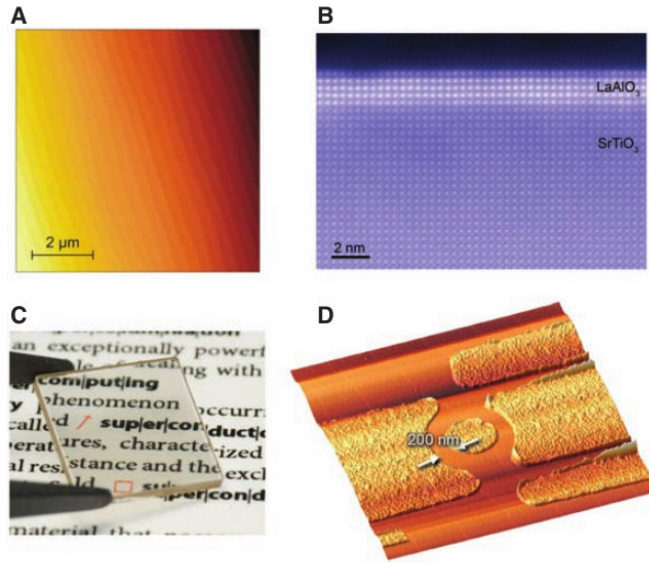


Fig. 1. Micrographs of $\text{LaAlO}_3\text{-SrTiO}_3$ heterostructures. (A) Top view of a $\text{LaAlO}_3\text{-SrTiO}_3$ bilayer containing eight monolayers of LaAlO_3 , taken by scanning force microscopy (figure courtesy of S. Paetel). (B) Cross-sectional view of a corresponding sample containing five monolayers of LaAlO_3 (figure courtesy of L. Fitting Kourkoutis and D. A. Muller). (C) Optical photograph of a complete sample (figure courtesy of G. Hammert and K. Wiedenmann). (D) Scanning force microscopy image of a conducting ring patterned by electron beam lithography into a $\text{LaAlO}_3\text{-SrTiO}_3$ structure [from (8)].

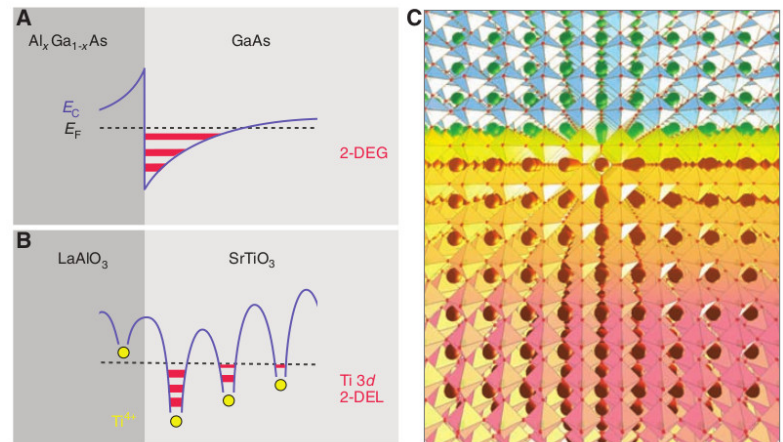


Fig. 4. (A and B) Comparison between two-dimensional electron systems generated at interfaces between standard semiconductors, for example, between GaAs and $\text{Al}_x\text{Ga}_{1-x}\text{As}$ (A) and between LaAlO_3 and SrTiO_3 (B). At the semiconductor interface, two-dimensional electronic subbands are formed within the quantum well generated by band bending. At the oxide interface, the two-dimensional bands are generated in the potential wells arising predominantly from the ionic charges. For the $\text{LaAlO}_3\text{-SrTiO}_3$ interface, these are 3d bands of Ti ions. The overall band bending lowers the electronic energies of the unit cells next to the interface, such that the mobile electron system that forms a two-dimensional electron liquid (2DEL) resides predominantly in the oxide planes next to the interface [after (46)]. (C) Illustration of the situation in (B): The LaAlO_3 is grown on top of the SrTiO_3 ; the mobile electron system is depicted in yellow.

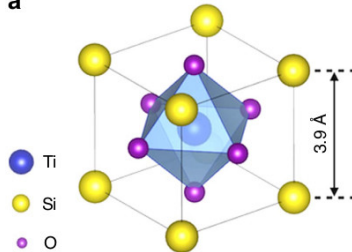
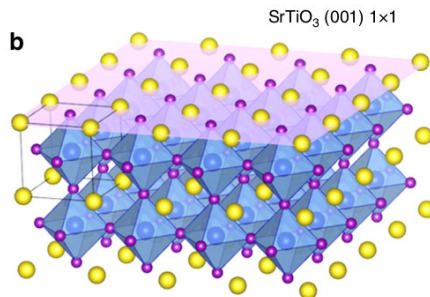
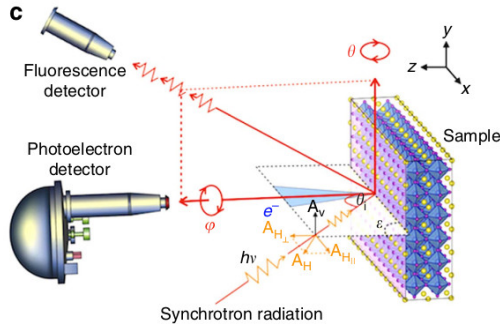
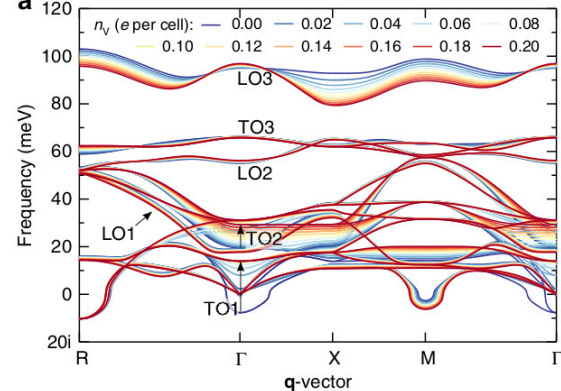
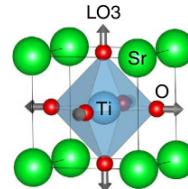
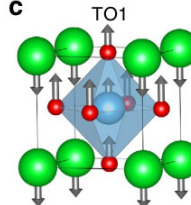
a**b****c****a****b****c**

Figure 3 | Theoretical phonon modes in cubic phase doped STO.

(a) Phonon dispersion at various electron doping levels n_v with our case corresponding to $n_v \sim 0.12$. The arrows indicate the TO1 and TO2 modes shifting as a function of n_v . The imaginary modes at the R- and M-points represent different octahedral rotation instabilities, whereas the one at the Γ -point in the undoped materials is the polar (quantum-paraelectric) instability. (b,c) Atomic displacements associated with the breathing LO3 mode at the R-point and the polar TO1 mode at the Γ -point, respectively.

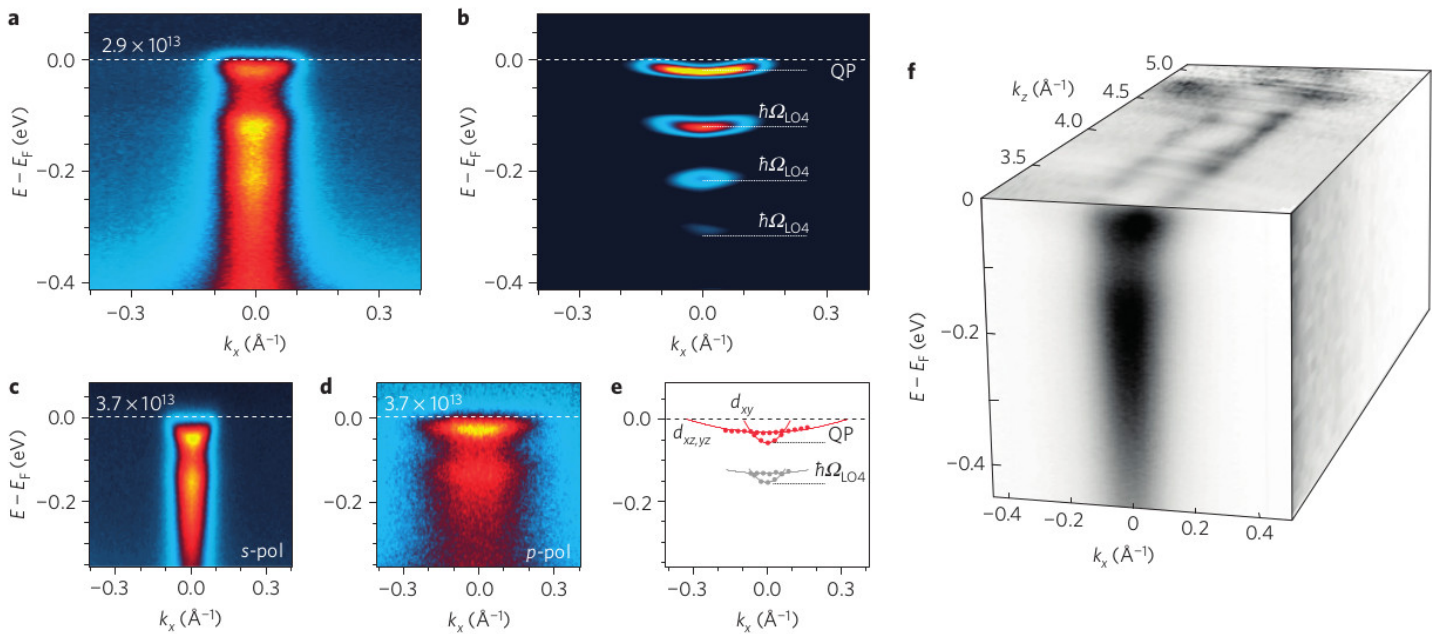


Figure 1 | A two-dimensional liquid of large polarons in SrTiO₃. **a,b,** Energy-momentum intensity map and curvature plot, respectively, for a 2DEL with $n_{2D} = 2.9 \times 10^{13}$ cm⁻² taken at a photon energy of 44 eV with s-polarization (E_F is the Fermi energy and k_x is the crystal momentum along [100]). Note the dispersive replica bands at higher binding energy arising from strong coupling to the LO₄ phonon branch of SrTiO₃ with energy $\hbar\Omega_{LO4}$ approximately 100 meV. **c,d,** Data taken on a sample with $n_{2D} = 3.7 \times 10^{13}$ cm⁻² using s- and p-polarized light, respectively, with a photon energy of $\hbar\nu = 85$ eV to selectively excite the light xy and heavy xz/yz orbitals. **e,** Dispersion of the main and first replica bands extracted from the data in **c** and **d**. **f,** Photon-energy-dependent measurements showing the lack of dispersion along k_z . All data were measured in the second Brillouin zone to avoid the minimum of the matrix elements at normal emission.

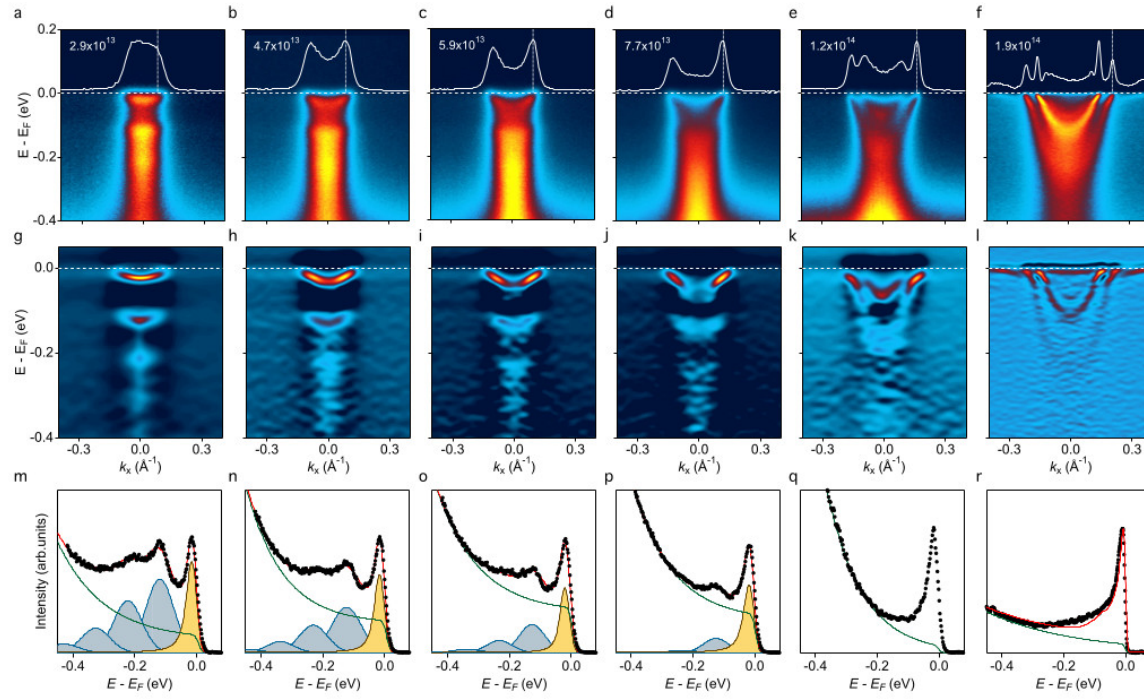


Figure 13. (a)–(f) ARPES spectra of the surface state on STO(001) acquired as a function of increasing carrier density. The images are cuts through the Γ point along (100) direction. The number on each panel is the 2D carrier density calculated from the Fermi surface size, assuming each band crossing the Fermi level is spin-degenerate. (g)–(l) The same spectra enhanced using the 2D curvature method [114] in order to clarify the replica bands. (m)–(r) Energy distribution curves evaluated at the Fermi momentum k_F of each corresponding image. The profiles in (g)–(j) are shown with fits of the main band and incoherent spectral tail to a Frank-Condon model with a single phonon mode of about 100 meV. Reprinted by permission from [68].

④ Phonon renormalization by electrons - Kohn anomalies

• phonon selfenergy

$$\textcircled{π} = \rightarrow_{q_i, i\omega} \text{ (loop diagram)} \rightarrow_{q_i, i\omega}$$

$$\sim |M_q|^2 \Pi_0(q, \omega)$$

↑ Lindhard Function

$$2k_F \text{ singularity: } \frac{\partial \Pi_0}{\partial q_r} \sim \ln |q - 2k_F|$$

→ Kohn anomaly in phonon dispersion

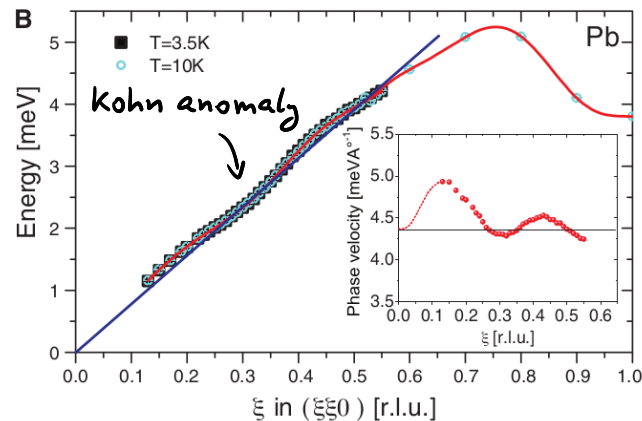
Energy Gaps and Kohn Anomalies in Elemental Superconductors

P. Aynajian,¹ T. Keller,^{1,2} L. Boeri,¹ S. M. Shapiro,³ K. Habicht,⁴ B. Keimer^{1*}

$$\text{~~~} = \text{~~~} + \text{~~~} \textcircled{π} \text{~~~}$$

$$-\mathcal{D} = -\mathcal{D}_0 + [-\mathcal{D}_0(-\pi)(-\mathcal{D})]$$

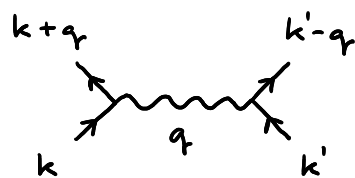
$$\mathcal{D}^{-1} = \mathcal{D}_0^{-1} - \Pi \quad \text{Dyson equation}$$



bars indicate the statistical errors. (B) Dispersion relation of the same phonon extracted from triple-axis data. (Inset) The phonon phase velocity (E/q) computed from the data. The blue line in (B) and the black line in the (B) inset represent the experimentally determined sound velocity (29).

⑤ Effective e-e interaction mediated by phonons - Cooper pairing

- diagrammatic element corresponding to effective e-e interaction



$$V_{\text{eff}}(q, i\nu) = |M_q|^2 \mathcal{D}(q, i\nu) \quad \& \text{ associated summations}$$

bare: $|M_q|^2 \left(\frac{1}{i\nu - \hbar\omega_q} - \frac{1}{i\nu + \hbar\omega_q} \right)$

CoCo Phenomena: $H_{\text{int}} = \frac{1}{2} \sum_{\substack{k k' q \\ \text{GG}'}} |M_q|^2 \left(\frac{1}{\varepsilon_k - \varepsilon_{k+q} - \hbar\omega_q} - \frac{1}{\varepsilon_k - \varepsilon_{k+q} + \hbar\omega_q} \right) \hat{c}_{k+q, G}^{\dagger} \hat{c}_{k'-q, G'}^{\dagger} \hat{c}_{k', G'} \hat{c}_{k, G}$

• Cooper instability

two-particle propagator diverges below $T_c \rightarrow$ condensation into Cooper pairs

